Journal of Non-Crystalline Solids xxx (xxxx) xxx–xxx

Contents lists available at ScienceDirect

Journal of Non-Crystalline Solids

journal homepage: www.elsevier.com/locate/jnoncrysol

# Crystallization behavior, densification and microwave dielectric properties of $MgO\text{-}Al_2O_3\text{-}SiO_2\text{-}TiO_2$ system glass-ceramics containing $V_2O_5$

Fei Liu[a], Xianpei Huang[b], Jingjing Qu[a,c], ChangLai Yuan[b,*], Guohua Chen[b], Ruofei Ma[b]

[a] Guangxi Key Laboratory of Manufacturing System and Advanced Manufacturing Technology, Guilin University of Electronic Technology, Guilin 541004, PR China
[b] Guangxi Key Laboratory of Information Materials, Guilin University of Electronic Technology, Guilin 541004, PR China
[c] Department of Computer Science and Engineering, Guilin University of Aerospace Technology, Guilin 541004, PR China

## ARTICLE INFO

*Keywords:*
Glass-ceramics
Two-step heat treatment
Dielectric properties
$V_2O_5$
Crystallization

## ABSTRACT

Glass-ceramics with a mass fraction composition (wt%) of $19MgO\text{-}23Al_2O_3\text{-}53SiO_2\text{-}4TiO_2\text{-}xV_2O_5$ ($x$ = 2.5, 3 and 3.5, abbreviated as samples V2.5, V3 and V3.5) were prepared by two-step heat treatment of the parent glass at selected nucleation and crystallization temperatures for different holding time (2 h and 20 h), respectively. The effects of $V_2O_5$ on crystalline phases, microstructures and microwave dielectric properties of the glass-ceramics were investigated in detail. X-ray diffraction (XRD) analyses revealed that the main phases could be identified as $\alpha$-cordierite and $SiO_2$ phases, and also some amount of $\mu$-cordierite phase and a trace of $Al_2Si_4O_{10}$, $Mg(VO_4)_2$ and $TiO_2$ phases were also detected in all these glass-ceramics' XRD patterns. In addition, an appropriate $V_2O_5$ addition with 3.0–3.5 wt% was found to cause an increase in the content of the precipitated crystalline phases. Based on the EDM observation, a fraction of $Ti^{4+}$ and $V^{5+}$ ions were remained in the residual glass matrix of the crystallized specimens. Additionally, the microwave dielectric properties were closely depended on not only the different two-step heat treatment temperatures and holding time, but also the relative densities and degree of crystallization of the glass matrix. Wherein, the fully densified V3 glass-ceramic sample heat-treated at 850 °C/2 h + 950 °C/20 h exhibited a lower dielectric constant ($\varepsilon_r$) of ~3.79, a higher quality factor ($Q \times f$) of about 12,520 GHz (at 13.693 GHz) and a near-zero temperature coefficient of resonant frequency ($\tau_f$) of $\sim -5.4$ ppm/°C, which provided a promising candidate for LTCC applications.

## 1. Introduction

In recent years, low-temperature cofired ceramics (LTCC) play a decisive role as the base materials in the development of complex miniaturized circuits such as capacitors, resistors, and inductors etc. [1,2]. The LTCC materials are cofired with an inner electrode structure to produce a module, therefore, the sintering temperature must be lower than the melting point of the electrode. For example, in the case of Cu-(1083 °C) or Au-based (1061 °C) electrodes, the sintering temperature should be < 1000 °C. Additionally, the low temperature also enables the advantageous utilization for today's packaging concepts in microelectronic and microwave modules. As the representative LTCC materials, some glass-ceramic systems, such as the $MgO\text{-}Al_2O_3\text{-}SiO_2\text{-}GeO_2$ and $MgO\text{-}Al_2O_3\text{-}SiO_2\text{-}TiO_2$, not only have a good thermal conductivity and mechanical properties, but also do not react with the conductive materials [3,4]. Wherein, the glass mainly acts as a low temperature sintering aid, and the ceramic fillers help in enhancing mechanical strength and minimizing distortion.

On the other hand, the main phase in the glass-ceramic composites is the crystalline phase in which the relatively high crystalline phase content will make a positive contribution for the dielectric properties, while an excess of the residual glass phase can cause a significant increase of the dielectric loss. Thus, during the heat treatment process, to promote the degree of crystallization from glass system is extremely important. Some research suggests that not only complete densification, but also sufficient crystallization can be achieved through adding oxides as the sintering additives or nucleating agents into glass matrix [5–7]. As a typical sintering aid, $V_2O_5$ has also been researched in detail for some promising LTCC materials [8,9]. However, to the best of our knowledge, the effect of $V_2O_5$ on crystallization behavior of $MgO\text{-}Al_2O_3\text{-}SiO_2\text{-}TiO_2$ systems has not been investigated, and also no relevant research work has been taken out on the microwave dielectric properties of these glass-ceramic systems.

In this paper, we therefore investigate the effects of $V_2O_5$ addition on the crystallization, sintering behaviors and dielectric properties of a selected $MgO\text{-}Al_2O_3\text{-}SiO_2\text{-}TiO_2$ system. Wherein, an appropriate $V_2O_5$ addition was found to promote the degree of crystallization from glass phase and improve the dielectric properties such as obtaining the low

---

* Corresponding author.
*E-mail address:* yclguet@yahoo.com (C. Yuan).

https://doi.org/10.1016/j.jnoncrysol.2017.11.017
Received 29 September 2017; Received in revised form 26 October 2017; Accepted 9 November 2017

Please cite this article as: Liu, F., Journal of Non-Crystalline Solids (2017), http://dx.doi.org/10.1016/j.jnoncrysol.2017.11.017

dielectric constant ($\varepsilon_r$) and high quality factor ($Q \times f$), comparing with that of the Mg-Al-Si and/or Mg-Al-Ti based glass-ceramic form the pure MgO-$Al_2O_3$-$SiO_2$-$TiO_2$ system ($\varepsilon_r \sim 5.5$–$7.5$ and $Q \sim 500$–$1000$) [10,11]. Also, another aim of the present study was to analyze the effect of the addition of $V_2O_5$ on the nucleation and crystallization behaviors of MgO-$Al_2O_3$-$SiO_2$-$TiO_2$ glass powder through two-step heat treatment methods with the selected sintering temperatures and holding time. As a consequence, the proposed method promises a new glass-ceramic with low $\varepsilon_r$ and high $Q \times f$ value on the MgO-$Al_2O_3$-$SiO_2$-$TiO_2$-$V_2O_5$ systems, which seem to be more promising for applications in LTCC modules than glass and ceramic mixtures.

## 2. Experimental procedure

MgO-$Al_2O_3$-$SiO_2$-$TiO_2$-$V_2O_5$ (Mg-Al-*Si*-Ti-V) glass with the composition of 19 wt% MgO, 23 wt% $Al_2O_3$, 53 wt% $SiO_2$, 4 wt% $TiO_2$ and $x$ wt% $V_2O_5$ ($x$ = 2.5, 3 and 3.5, abbreviated as samples V2.5, V3 and V3.5) were prepared by melting powders containing appropriate amounts of reagent grade MgO, $Al_2O_3$, $SiO_2$, $TiO_2$ and $V_2O_5$ in alumina crucibles at 1500 °C for 2 h, and then quenched in distilled water. The cullet was pulverized and wet-milled for 50 h, and then sieved through a 100 mesh. To prepare the bulk samples, the obtained glass powders were granulated with 5% PVA solution as a binder and pressed uniaxially at about 180 MPa to make a pellet with 12 mm in diameter and 1 mm and/or 6 mm in height. The pellets were heat-treated at 930–970 °C for 2 h/20 h after being held at 820–880 °C in air for 2 h (two-step heat treatment).

The densities of the heat-treated specimens were measured using Archimedes' principle using distilled water as medium. The glass crystallization behavior was characterized by using differential scanning calorimeter (DSC, Model STA 499C, Netzsch). Approximately 10 mg of ground glass was used for DSC measurement at a rate of 10 °C/min up to 1200 °C. The crystalline phases and crystallization behaviors of the specimens were determined using an X-ray diffractometer (XRD, CuKa, 1.54059 Å, Model D8-Advance, Bruker, Germany), and the XRD patterns analysis did not reveal any crystal phase for the Mg-Al-*Si*-Ti-V glass powders, as shown in Fig. 1. The microstructures of the glass-ceramics were observed using field-emission scanning electron microscope (SEM, Model S-4800, Hitachi, Japan). Moreover, the relative dielectric constant ($\varepsilon_r$) and quality factor ($Q \times f$, $Q$ = 1/dielectric loss and $f$ = resonant frequency) of the sintered specimens were measured in the range of 13.3–14.2 GHz by the $TE_{01\delta}$ mode dielectric resonator technique using a vector network analyzer (E5230C, Agilent Co., CA, 10 MHz to 40 GHz) in the $S_{21}$ transmission mode. In addition, the temperature coefficient of the resonant frequency ($\tau_f$) were measured by the open cavity method using an invar cavity, and calculated through the formula as follows [12]:

$$\tau_f = \frac{\Delta f_0}{f_0 \Delta T} = \frac{f_{75} - f_{25}}{f_{25} \times 50} \tag{1}$$

where $f_{75}$ and $f_{25}$ represent the resonant frequencies at 75 °C and 25 °C, respectively.

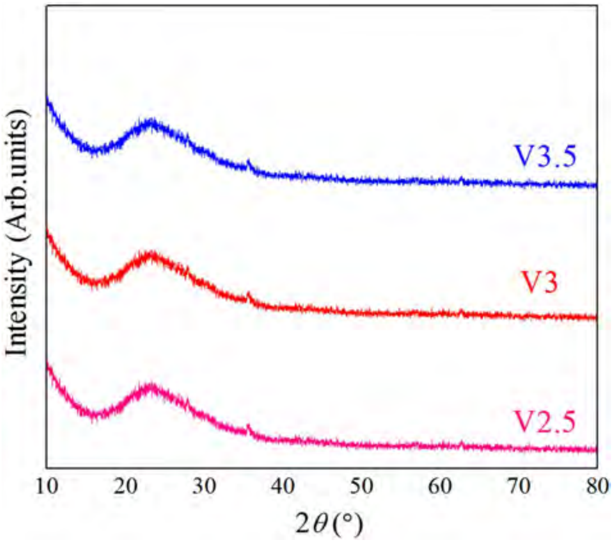

**Fig. 1.** X-ray diffraction patterns of Mg-Al-*Si*-Ti glass added with different $x$ wt% $V_2O_5$ without heat treatment.

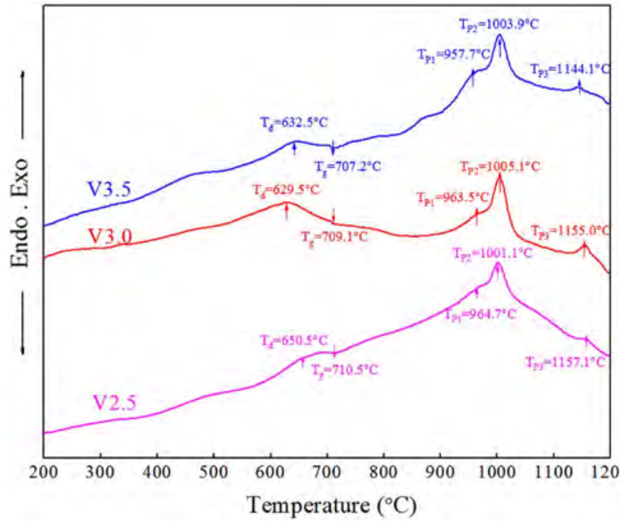

**Fig. 2.** DSC measurement results for the Mg-Al-Si-Ti glass added with different amounts of $V_2O_5$.

## 3. Results and discussion

To determine the crystallization behaviors of the Mg-Al-*Si*-Ti glasses with different addition amounts of $V_2O_5$, the typical events occurred during the transformation from glass to glass-ceramics are clearly visible in the DSC curve determined at a heating rate of 10 °C/min, as shown in Fig. 2. For all the Mg-Al-*Si*-Ti-V glass powders, the glass softening point temperatures ($T_d$) are noticed at approximately 629–651 °C, and the obscure broadening endothermic peaks ($T_g$) can also be observed in the temperature range between 707 °C and 711 °C due to glass transition. However, this endothermic peak is weaker, so the values of the onset temperature for the nucleation should be determined a range from $T_g$ to the first exothermic peak ($T_{p1}$) [13]. Therefore, the selected reasonable nucleation temperatures are 820–880 °C in this work.

Additionally, one broadening ($T_{p1}$) and one sharp exothermic ($T_{p2}$) peaks corresponding to glass crystallization at around 957–965 °C and 1001–1006 °C are observed in these glass powders' DSC curves, respectively. Generally, these obvious exothermic peaks are attributed to the main crystallization of glass. Moreover, this is followed by third exothermic transformation ($T_{p3}$) corresponding to glass crystallization at around 1144–1158 °C. On the other hand, because the sintering temperature of the commercial glass-ceramics should be lowered to below 1000 °C, and the practical crystallization temperature is usually found to be slightly lower than theoretical $T_p$ (~ 50 °C) [13,14]. Thus, the selected reasonable crystallization temperature is in the temperature range of 930–970 °C for the present glass-ceramic systems. In addition, according to our previous work researched in MgO-$Al_2O_3$-$SiO_2$-$TiO_2$-$B_2O_3$ (under review), the relative densities and quality factor ($Q \times f$) of the specimens heat-treated at crystallization temperatures for 2 h and 20 h were relatively superior than those of the specimens for other hold time (1 h, 5 h, 10 h and 30 h). Hence the hold time at nucleation and crystallization temperature are set to as 2 h and 2 h/20 h,

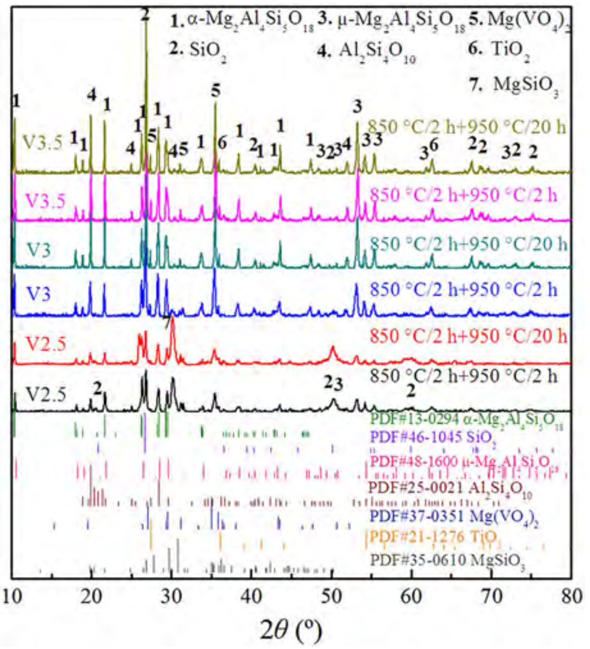

**Fig. 3.** XRD patterns of Mg-Al-Si-Ti-$x$ wt% $V_2O_5$ ($2.5 \le x \le 3.5$) glass-ceramics specimens obtained after a two-step heat treatment (850 °C/2 h + 950 °C/2 h and 850 °C/2 h + 950 °C/20 h).

respectively, in this work.

Fig. 3 presents the XRD patterns of the Mg-Al-*Si*-Ti-$x$ wt% $V_2O_5$ ($2.5 \le x \le 3.5$) glass-ceramics heat-treated in two steps (850 °C/2 h + 950 °C/2 h and 850 °C/2 h + 950 °C/20 h). From Fig. 3, it is clearly found that the predominant crystalline phases in samples V2.5 at different holding time (2 h and 20 h) are $\alpha$-cordierite (JCPDS#13–0294) and $SiO_2$ (JCPDS#46–1045), and some amount of $\mu$-cordierite phase (JCPDS#48–1600) appears. In addition, a trace of $MgSiO_3$(JCPDS#35–0610), $Al_2Si_4O_{10}$ (JCPDS#25–0021), $Mg(VO_4)_2$ (JCPDS#37–0351) and $TiO_2$ (JCPDS#21–1276) phases are also detected at these XRD patterns. In samples V3 and V3.5, the main phases are still $\alpha$-cordierite and $SiO_2$, and both their XRD peaks intensities evidently increase, compared with that of in samples V2.5, and the phase content of the samples held on 20 h is higher than that of the samples held on 2 h in the same heat treated temperatures. This result means that a prolonged hold time (20*h*) and an appropriate $V_2O_5$ addition can promote the crystallization in the Mg-Al-*Si*-Ti glass matrix. Additionally, the $\mu$-cordierite and $Mg(VO_4)_2$ phases also have a slight increase, and $Al_2Si_4O_{10}$ and $TiO_2$ still exist, while the $MgSiO_3$ phase gradually decreases with increasing $V_2O_5$ addition. Moreover, it is found that, comparing the DSC (see Fig. 2) and XRD results, the first and second exothermic peaks in the DSC curves should be assigned to the crystallization of $\alpha$-cordierite and $SiO_2$, respectively. However, it is worth noting that there are only two exothermic peaks corresponding to the main crystalline phases, and no other exothermic peaks can match with the rest of second phases (see Fig. 2). This is more likely to be resulted from the reaction between the main crystalline phases and/or $V_2O_5$ and amorphous glass phase, which is confirmed by the XRD patterns for these samples after a longer heat-treatment process, comparing with the results of DSC test [15,16].

On the other hand, Fig. 4 shows the XRD patterns of V3 specimens that are heat-treated at 930–970 °C for 20 h after being held at 820–880 °C for 2 h. It can be seen from that the XRD curves exhibit a similar profile for all samples sintered at different heat-treatment temperatures, which implies that the phase compositions of the V3 glass-ceramics are not sensitive to the nucleation temperatures from 820 °C to 880 °C and crystallization temperatures from 930 °C to 970 °C. But, it is noteworthy that the XRD peaks intensities of the main phases ($\alpha$-cordierite and $SiO_2$) for the V3 sample heat-treated at 850 °C/2 h + 950 °C/20 h are relative higher than that of other V3 specimens. The remained phase compositions in V3 samples also illustrate that a certain content of $V_2O_5$ addition can broaden the glass transition and crystallization temperature ranges for the investigative Mg-Al-*Si*-Ti glass matrix in this work.

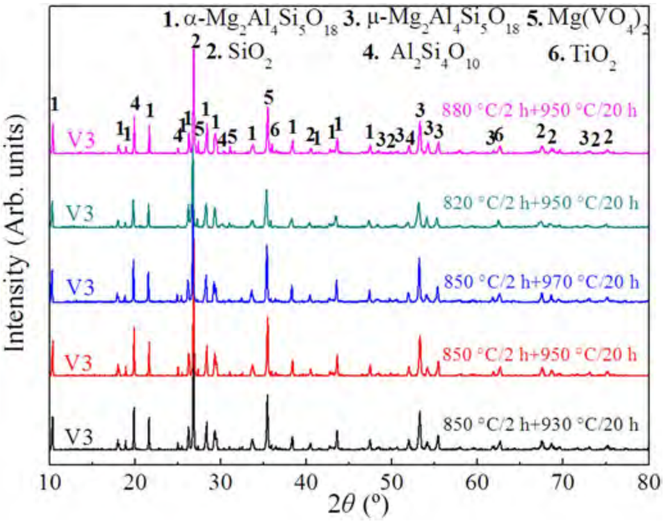

**Fig. 4.** XRD patterns of V3 samples heat-treated at 820–880 °C/2 h + 930–970 °C/20 h.

SEM micrographs of Mg-Al-Si-Ti-$x$ wt% $V_2O_5$ ($2.5 \le x \le 3.5$) specimens heat treated in a two steps are shown in Fig. 5. As shown in Fig. 5(a), sample V2.5 heat-treated at 850 °C/2 h + 950 °C/20 h has more residual glass phase (amorphous region). With increasing $V_2O_5$ addition [see Fig. 4(b)–(d)], the crystallization of the specimens V3 increases, and a certain content of $V_2O_5$ addition can indeed improve the content of the precipitated crystalline phases, which is in agreement with the results of the XRD patterns given in Fig. 3. In addition, the grain boundaries are relatively clearly visible through the prolonged hold time (20 h) in the same heat treatment temperatures, comparing with that of the V3 sample held on 2 h, as shown in Fig. 5(e). Moreover, from Fig. 5(f), it can be seen that a certain number of pores of the V3.5 specimen increase in a same heat-treatment process (850 °C/2 h + 950 °C/20 h), which will affect the relative density results and microwave dielectric properties in the present glass-ceramic systems.

To obtain more detailed information about the phase compositions, sample V3 heat-treated at 850 °C/2 h + 950 °C/20 h are investigated by element distribution mapping (EDM) in Fig. 6. It can be observed that two colors grains, the white and the dark-grey, coexist in this sample [see Fig. 6(a)]. EDM image derived from Fig. 6(a) shows that the white grains are mainly composed of Mg (wathet), Al (fushcia), Si (red) and O (green), as shown in Fig. 6(b). Therefore, combined to the XRD patterns results (Fig. 3), we deduce the white grains should be the $\alpha$-cordierite phase. For the dark-grey grains regions, there are more or less $Ti^{4+}$ (yellow) and $V^{5+}$ (orange) ions diffused in these grains' surfaces. It is noteworthy that other types of grains are hardly found in the surface of this specimen, and therefore other phases' particles are covered by the coexistence of the dark-grey grains and residual glass phase containing the dissociative $Ti^{4+}$ and $V^{5+}$ ions [17]. Also, as can be seen from the EDS data in Fig. 6(c), the whole area resulted from Fig. 6(b) reveals the rich- Mg, Si, Al and O element, whereas a small amount of $Ti^{4+}$ and $V^{5+}$ ions dissolves. It also implies that not all $Ti^{4+}$ and $V^{5+}$ ions incorporate into the formation of the crystalline phase in these glass-ceramic systems.

The dielectric constant ($\varepsilon_r$), quality factor ($Q \times f$), temperature coefficient of resonant frequency ($\tau_f$) and linear shrinkage rate are investigated for the V2.5, V3 and V3.5 glass-ceramic samples heat-treated at 850 °C/2 h + 950 °C/20 h, and the results are shown in Fig. 7.

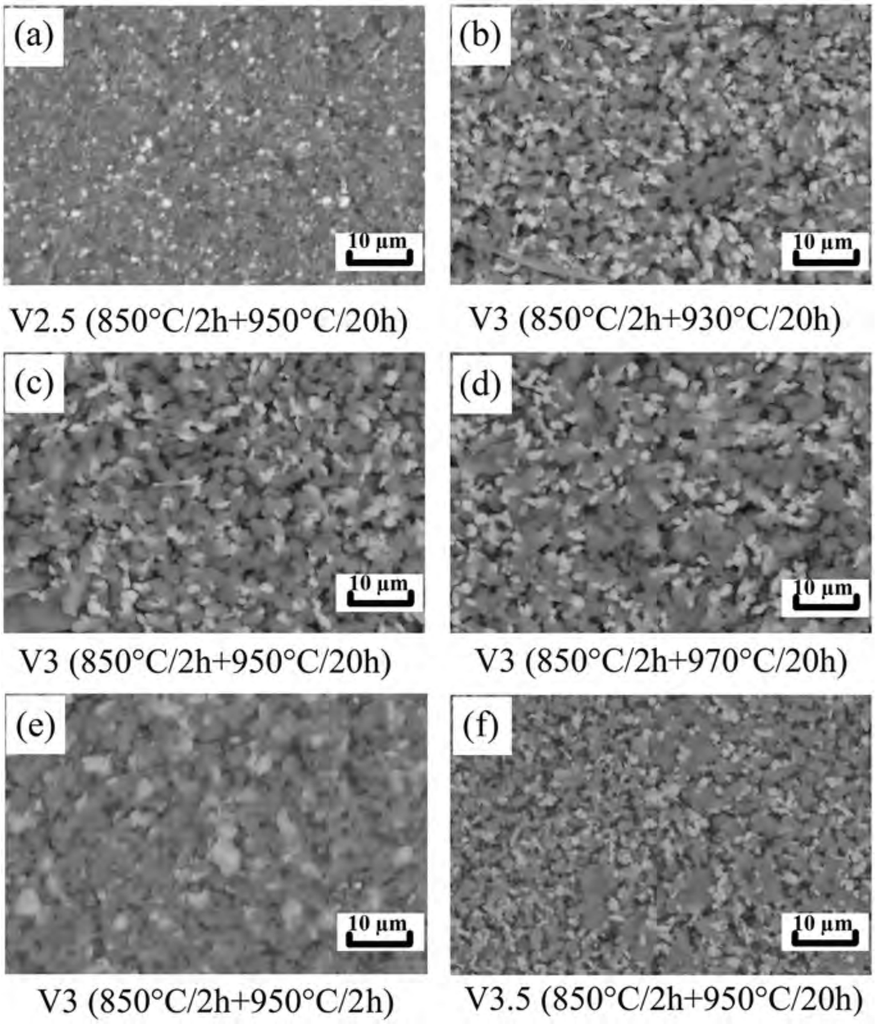

**Fig. 5.** SEM (× 5000) micrographs of Mg-Al-Si-Ti-$x$ wt% $V_2O_5$ ($2.5 \le x \le 3.5$) specimens produced using a two-step heat treatment.

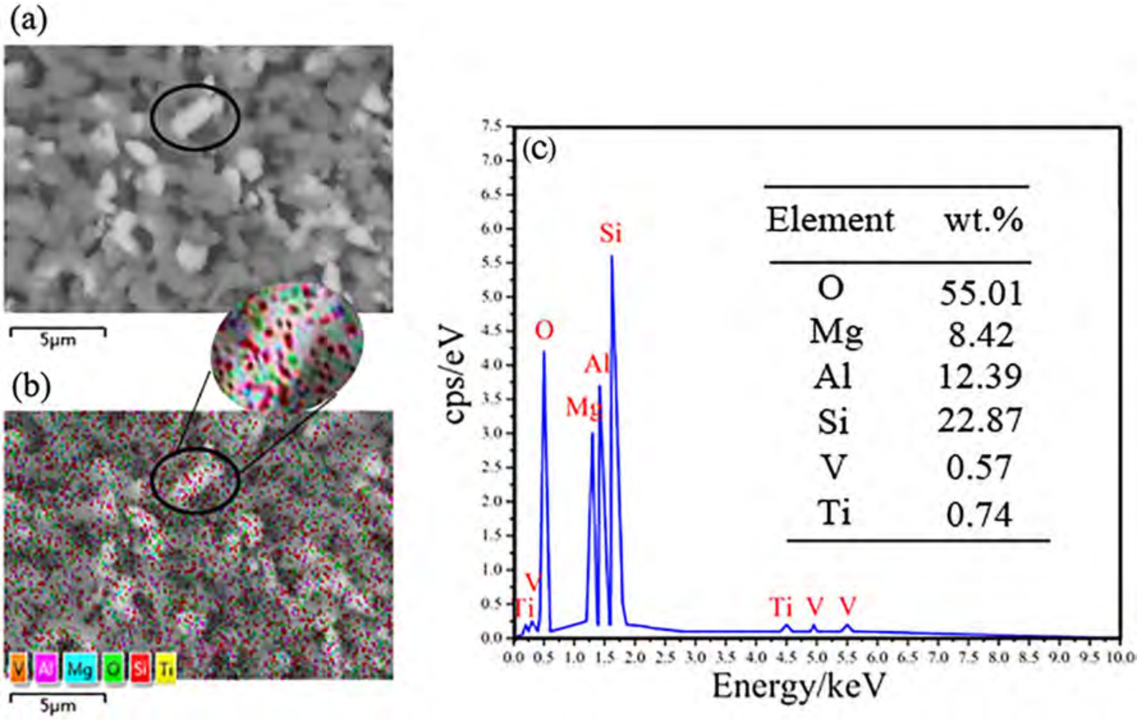

| Element | wt.% |
|---|---|
| O | 55.01 |
| Mg | 8.42 |
| Al | 12.39 |
| Si | 22.87 |
| V | 0.57 |
| Ti | 0.74 |

**Fig. 6.** (a) SEM (× 10,000) micrographs, (b) element distribution mapping (EDM) and (c) results of EDM analysis of sample V3 heat-treated at 850 °C/2 h + 950 °C/20 h.

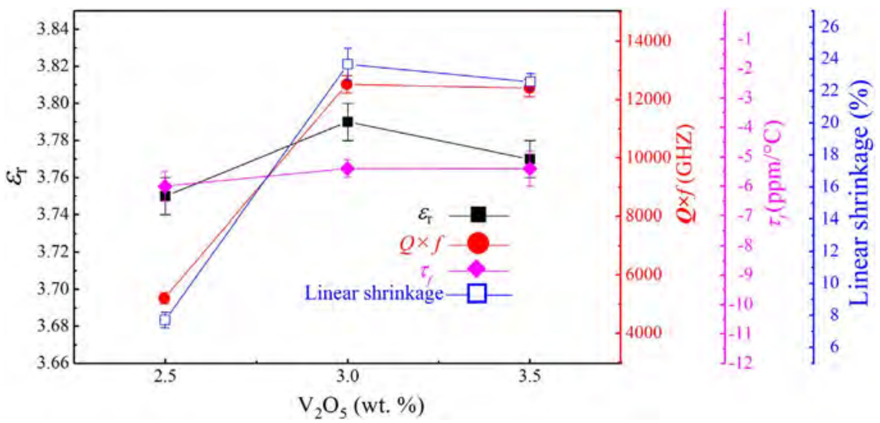

**Fig. 7.** Changes in $\varepsilon_r$, $Q \times f$, $\tau_f$ values and linear shrinkage of V2.5-V3.5 samples heat-treated at 850 °C/2 h + 950 °C/20 h.

**Table 1**
Other representative microwave dilelectric properties of the glass-ceramics V3 after two-step heat-treatment process.

| Heat-treatment (°C/h + °C/h) | $\varepsilon_r$ ± 0.1 | $Q \times f$ (GH$_Z$) ± 50 | $f$ (GH$_Z$) ± 0.005 | $\tau_f$ (ppm/°C) ± 0.1 |
|---|---|---|---|---|
| 850/2 + 930/20 | 3.71 | 9780 | 13.679 | − 4.71 |
| 850/2 + 970/20 | 3.75 | 10,330 | 13.814 | − 3.94 |
| 820/2 + 950/20 | 3.69 | 10,920 | 13.740 | − 5.53 |
| 880/2 + 950/20 | 3.78 | 8950 | 14.104 | − 6.54 |
| 850/2 + 950/2 | 3.72 | 8330 | 13.689 | − 6.82 |

Generally, a glass-ceramic material's $\varepsilon_r$ value is affected by its porosity, density, and the degree of crystallization [18–20]. It can be seen that the $\varepsilon_r$ value (3.74–3.79) does not change considerably with different $V_2O_5$ addition in present glass-ceramic systems. While the changed trends of $\varepsilon_r$ value of specimens still agree with the trends of their linear shrinking percentage in Fig. 7. The larger linear shrinking rate means the higher relative density, and the less porosity in sample's interior structure. It is also confirmed that the maximum $\varepsilon_r$ ~3.79 can be obtained for the V3 sample heat-treated at 850 °C/2 h + 950 °C/20 h due to the higher compactness and degree of crystallization, as shown in Fig. 3 and Fig. 5. On the other hand, the changes in $Q \times f$ values also exhibit a tendency similar to those of their linear shrinking percentage with different $V_2O_5$ addition in Fig. 7. As is well-known, the $Q \times f$ of glass-ceramics is more dependent on the relative density and the degree of crystallization of the glass matrix as well. Additionally, in addition to these factors, a lower $Q \times f$ value ~5200 GHz in V2.5 specimen heat-treated at 850 °C/2 h + 950 °C/20 h is also probably due to a large glass network formed in the materials [see Fig. 5(a)]. The glass network profoundly absorbs the microwave power at high frequency regime, causing a dramatic degradation of the quality factor [21]. Moreover, the similar $\tau_f$ value around − 5.39 ppm/°C to − 6.01 ppm/°C is obtained for the V2.5–V3.5 glass-ceramic specimens prepared by the same heat-treatment conditions.

Table 1 shows other representative microwave dielectric properties of the glass-ceramics V3 after two-step heat-treatment process. In this paper, we originally tried to adjust the heat-treatment temperatures and hold time to improve the $Q \times f$ value through two-step heat-treatment conditions. However, no significant improvement in the $Q \times f$ value can be achieved with the increase in nucleation temperatures ~880 °C and crystalline temperature ~970 °C. In addition, a shorter sintering time ~2 h can not effectively enhance the $Q \times f$ value of the V3 glass-ceramics as well. Therefore, the better two-step heat-treatment process for Mg-Al-*Si*-Ti-$x$ wt% $V_2O_5$ ($2.5 \le x \le 3.5$) glass-ceramics should be the 850 °C/2 h + 950 °C/20 h process.

## 4. Conclusion

In this study, the $MgO$-$Al_2O_3$-$SiO_2$-$TiO_2$-based (M-A-S-T) glasses adding $V_2O_5$ of 2.5–3.5 wt% were prepared by two-step heat-treatment. The fabricated glass-ceramics were characterized in terms of sinter-crystallization behavior and microwave dielectric properties. X-ray diffraction analyses revealed that the main phases consisted of $\alpha$-cordierite and $SiO_2$ could be detected, and also some amount of $\mu$-cordierite phase and a trace of $Al_2Si_4O_{10}$, $Mg(VO_4)_2$ and $TiO_2$ phases were also defined as the crystalline phases for all the glass-ceramics' XRD patterns. Wherein, the addition of a small amount, 3.0–3.5 wt%, of $V_2O_5$ was found to increase the degree of crystallization after the two-step heat treatment process, which resulted in improved $Q \times f$ values. Also, $Ti^{4+}$ and $V^{5+}$ ions had been confirmed to remain in the residual glass matrix of the crystallized specimens. Moreover, $\varepsilon_r$ and $Q \times f$ values showed the markedly dependent on the relative density and the degree of crystallization of the glass matrix. In particular, the glass-ceramic specimen with 3.0 wt% $V_2O_5$ addition nucleated at 850 °C/2 h and crystallized at 950 °C/20 h showed a better microwave dielectric properties of $\varepsilon_r$ ~3.79, $Q \times f$ ~12,520 GHz (at 13.693 GHz) and $\tau_f$ ~− 5.40 ppm/°C.

## Acknowledgement

Financial support from the National Natural Science Foundation of China (Grant No. 11464006) and the Middle-aged and Young Teachers of the College and/or Universities for Basic Ability Promotion Project in Guangxi of China (Grants No. KY2016YB534) is gratefully acknowledged by the authors.

## References

[1] A. Baker, M. Lanagan, C. Randall, E. Semouchkina, G. Semouchkin, K.Z. Rajah, R. Eitel, K.Z. Rajab, R. Mittra, S. Rhee, Int. J. Appl. Ceram. Technol. 2 (2005) 514–520.
[2] H.I. Hsiang, L.T. Mei, S.W. Yang, W.C. Liao, F.S. Yen, Ceram. Int. 37 (2011) 2453–2458.
[3] V.V. Golubkov, O.S. Dymshits, A.A. Zhilin, T.I. Chuvaeva, A.V. Shashkin, Glas. Phys. Chem. 30 (2004) 300–310.
[4] M.H. Lim, J.H. Park, H.G. Kim, M.J. Yoo, Proc. IEEE Intl. Conf. Properties Appl. Dielectric Mater. 2 (2003) 757–760.
[5] G.H. Chen, X.Y. Liu, J. Alloys Compd. 431 (2007) 282–286.
[6] S.B. Sohn, C.S. Young, J. Non-Cryst. Solids 282 (2001) 221–227.
[7] Y. Imanaka, Multilayered Low Temperature Cofired Ceramics (LTCC) Technology, Springer, Berlin, 2005.
[8] Z.H. Yao, H.X. Liu, Z.Y. Shen, Z.Z. Chen, Z.H. Wu, H.T. Yu, M.H. Cao, Mater. Res.

Bull. 41 (2006) 1972–1978.
[9] Q.L. Zhang, H. Yang, J.X. Tong, Mater. Lett. 60 (2006) 1188–1191.
[10] J.G. Wang, W. Chen, L. Luo, J. Alloys Compd. 464 (1–2) (2008) 440–445.
[11] S. Rajesh, H. Jantunen, M. Letz, S.P. Willhelm, Int. J. Appl. Ceram. Technol. 9 (1) (2012) 52–59.
[12] T. Nishikawa, K. Wakino, H. Tamura, H. Tanaka, Y. Ishikawa, IEEE MTT-S Int. Microw. Symp. Dig. 1 (1987) 277–280.
[13] X.H. Zhou, B. Li, S.R. Zhang, H.Y. Ning, J. Mater, Sci.: Mater. Electron. 20 (2009) 262–266.
[14] X.P. Huang, C.L. Yuan, X.Y. Liu, F. Liu, Q. Feng, J.W. Xu, C.R. Zhou, G.H. Chen, J. Non-Cryst. Solids 459 (1) (2017) 123–129.
[15] U. Došler, M.M. Kržmanc, D. Suvorov, Ceram. Int. 38 (2012) 1019–1025.
[16] G. Carl, T. Höche, B. Voigt, Phys. Chem. Glasses 43C (2002) 256–258.
[17] H.J. Wang, B.T. Li, H.X. Lin, W. Chen, L. Luo, Int. J. Appl. Glas. Sci. 5 (4) (2014) 436–442.
[18] S. Banijamali, T. Ebadzadeh, J. Non-Cryst. Solids 441 (2016) 34–41.
[19] B.K. Choi, S.W. Jang, E.S. Kim, Mater. Res. Bull. 67 (2015) 234–238.
[20] S. Jo, S.G. Kang, J. Nanosci. Nanotechnol. 13 (2013) 3542–3545.
[21] K.C. Feng, C.C. Chou, L.W. Chu, H. Chen, Mater. Res. Bull. 47 (2012) 2851–2855.